

## Single Phase Transformerless Grid-Tied Inverter with Maximum Power Point Tracking for Solar Photovoltaic Roof-Top Systems

Shruthi K J\*, Rajashekar P Mandi\*, Pradeep K\*, Viswanatha C\*\* and Giridhar Kini P\*\*\*

*The key requirements for the control of the solar photovoltaic (SPV) energy conversion systems are to achieve very fast yet quite accurate tracking of the maximum power point under rapidly changing environmental conditions and to obtain efficient unperturbed tracking operation under steady environmental conditions. In this work, a high-performance Maximum Power Point Tracking (MPPT) technique, based on one cycle control (OCC), is proposed to meet these challenging requirements. This paper proposes single phase z-source inverter with maximum power point tracking using OCC for solar photovoltaic power generation. OCC is based on output current adjustment according to the voltage of photovoltaic array so as to extract the maximum power from it. A 1 kW grid-tied roof-top system is designed using the OCC method for MPP. Analysis & simulation using MATLAB tool, is carried out to validate the proposed technique.*

**Keywords** *Grid-tied transformerless inverter, photovoltaic (PV) system, z-source network, Maximum power point tracking (MPPT), One Cycle Control (OCC)*

### 1.0 INTRODUCTION

The solar photovoltaic systems (SPV), based on their connectivity can be classified into two types: stand-alone systems and grid connected systems. Stand alone system is not connected to the national power grid. Grid connected Photovoltaic PV systems is suitable connected to grid and hence synchronization with grid is of primary importance. SPV systems both grid tied and off grid PV systems are now being looked upon as an option for power generating sources and installed for residential purposes.

A single phase grid connected system mainly consists of solar array, single phase power conditioning unit (inverter) , output filter (LC) and grid. The solar cells are connected in series-parallel configuration to match the required

voltage & power rating. The output from the inverter is sinusoidal and output current in phase with the utility and with unity power factor. In grid tied PV system, a transformer is connected between the inverter and grid which provides the much required isolation between grid and PV system. It also results in reduced leakage current levels between the PV system and ground and ensures direct dc current injection to grid (which causes saturation of distribution transformers) is eliminated [2]. However, these transformers have low operating frequencies, are bulky and expensive. Thus they reduce overall conversion efficiency. Hence transformerless inverter topologies [1-4] using solid state power electronic devices have generated research interests ensuring improved conversion efficiency, reduced cost and compact system. Though the use of solid state devices in the conversion circuits introduces harmonics in

\*Energy efficiency and Renewable Energy Division (ERED), Central Power Research Institute, Bangalore-560080.  
Email : shruthi.cpri@gmail.com, mandipri@cpri.in

\*\*Diagnostics Cables and Capacitors Division (DCCD), Central Power Research Institute, Bangalore-560080. Email : viswa@cpri.in

\*\*\*Professor, Electrical and Electronics Engineering Dept., Manipal Institute of Technology, Manipal. Email : giridhar.kini@manipal.edu

the output waveform which in turn brings down the efficiency of the converter, efforts have been made to bring down the harmonics through various control techniques.

In this paper, a simple low cost single stage inverter with maximum power point tracking (MPPT) control is proposed. The proposed topology can automatically adjust output power in accordance with the sunlight radiance level and provide sinusoidal current output to the grid. It will also include the following features:

- a) Constant switching frequency
- b) Simple power circuit with single stage conversion
- c) Accurate maximum power tracking control
- d) Reduced output leakage current harmonics with high power factor ( $\approx 1$ ).
- e) Improved conversion efficiency and low cost.

A proposed block diagram for single phase grid tied PV system which uses transformerless z-source inverter (ZSI) topology [5-8] and one cycle control (OCC) for MPPT control is as shown in Figure 1.

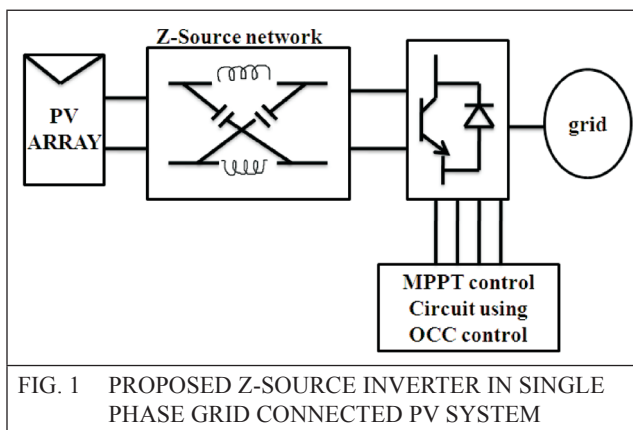


FIG. 1 PROPOSED Z-SOURCE INVERTER IN SINGLE PHASE GRID CONNECTED PV SYSTEM

Solar PV cell modeling is described in section 2. Then construction & operation of single phase ZSI is described in section 3. The OCC technique for MPPT control [9-10] is explained in section 4 followed by stability analysis and results in sections 5 & 6 respectively. Finally, a brief conclusion of the proposed single phase ZSI using OCC for MPPT is given in section 7.

## 2.0 SOLAR CELL/ PV ARRAY MODELING

A solar cell comprises of light- generating current source, diode, series resistance and parallel resistance as shown in Figure 2.

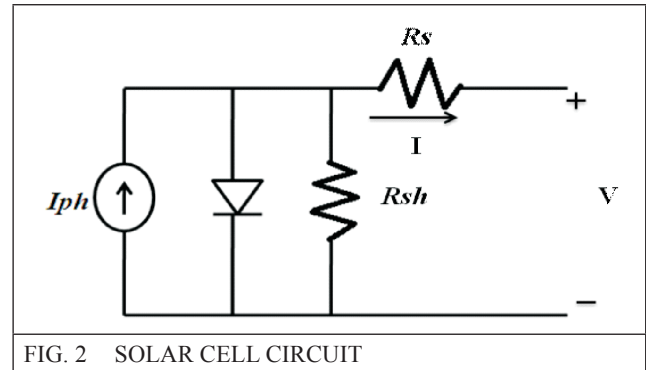


FIG. 2 SOLAR CELL CIRCUIT

Terminal equation for current- voltage of the solar cell is given by:

$$I = I_{ph} - I_{sat} \left\{ \exp \left( \frac{V + IR_s}{k_o} \right) - 1 \right\} - \frac{V + IR_s}{R_{sh}} \quad \dots(1)$$

where

$$k_o = AKT/q$$

$I, V$  - cell output current and voltage (V)

$I_{ph}$  - light generated current (A)

$I_{sat}$  - cell reverse saturation current (A)

$A$  - ideality factor ( $\approx 1$ );

$k$  - Boltzmann's constant ( $= 1.3805 \times 10^{-23}$  N.m/K)

$T$  - cell temperature ( $^{\circ}C$ )

$q$  - electronic charge ( $= 1.6 \times 10^{-19}$  C)

$R_s$  - series resistance ( $\Omega$ )

$R_{sh}$  - shunt resistance ( $\Omega$ ).

The equivalent circuit of solar cells arranged in  $N_p$  (parallel) and  $N_s$  (series) as shown in Figure 3, and mathematical equation having the array current-voltage is as given below:

$$I = N_p I_{ph} - N_p I_{sat} \left\{ \exp \left( \frac{V_{sa}}{N_s k_o} + \frac{I_{sa} R_s}{N_p k_o} \right) - 1 \right\} - \frac{1}{R_{sh}} \left( \frac{V_{sa}}{N_s} + \frac{I_{sa} R_s}{N_p} \right) \quad \dots(2)$$

where  $N_p$  is the number of parallel modules. Each module is composed of  $N_s$  cells connected in series.  $N_p I_{ph}$  corresponds to the short circuit current of the solar array. The general characteristic curves of the solar array are shown in Figure 4.

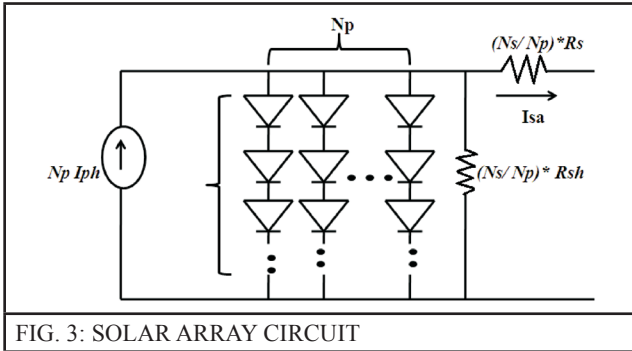


FIG. 3: SOLAR ARRAY CIRCUIT

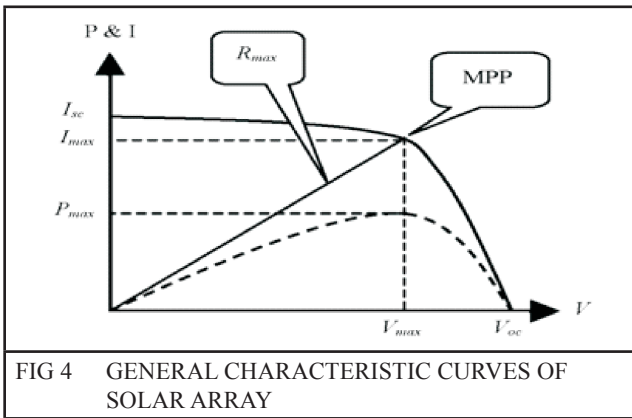


FIG 4 GENERAL CHARACTERISTIC CURVES OF SOLAR ARRAY

### 3.0 Z-SOURCE INVERTER

A Z- source inverter (ZSI) circuit has many advantages over other traditional inverters and are as listed below:

- Can produce any desired output a voltage (less than/ greater than the line voltage), regardless of the input voltage, thus eliminating need for another dc-dc converter.
- Provide ride-through during voltage sags without any additional circuits.
- Improve power factor reduces harmonic current and common-mode voltage.

ZSI impedance network using single phase full-bridge inverter is as shown in Figure 5.

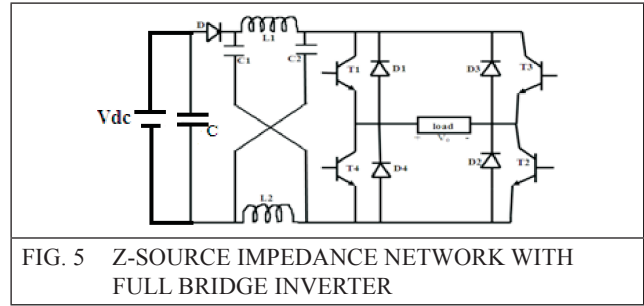


FIG. 5 Z-SOURCE IMPEDANCE NETWORK WITH FULL BRIDGE INVERTER

### 3.1 CONSTRUCTION & OPERATION

ZSI has impedance network on its dc side, connecting source to inverter. The unique impedance network consists of passive components (inductors and capacitors) which gives a single-stage conversion. The impedance network forms a second order filter which handles undesirable voltage sags of the dc voltage source. It reduces the inrush current and harmonics in the current because of two inductors in z-source network.

The presence of two inductors and capacitors in z-source network, allows both the switches in the same phase leg in ON state, simultaneously, called as “shoot through state”. A diode (D) is required to prevent the discharge of charged capacitor through the source. ZSI has 5 possible switching states: active / non-shoot through state, zero states and shoot through states.

Equation representing shoot through mode for ZSI is:

$$V_{L1}=V_{C1}; V_{L2}=V_{C2} \quad \dots(3)$$

It is assumed that the impedance network is a symmetric network ( $C_1=C_2=C$  and  $L_1=L_2=L$ ), thus it can be observed that  $V_{L1}=V_{L2}=V_L$  and  $I_{L1}=I_{L2}=I_L$  and the DC link voltage across the inverter bridge during shoot through interval is given in (4)

$$V_i=0 \quad \dots(4)$$

The inductor voltages in two modes are as given below:

$$\text{Shoot through mode: } V_L=V_C \quad \dots(5)$$

$$\text{Non-shoot through mode: } V_L=V_{dc}-V_C \quad \dots(6)$$

The average inductor voltage over one switching period must be zero.

$$V_L = \frac{T_0 \times V_c + T_1 \times (V_{dc} - V_c)}{T} = 0 \quad \dots(7)$$

$$\frac{V_c}{V_{dc}} = \frac{T_1}{T_1 - T_0} \quad \dots(8)$$

$V_L$ -inductor voltage (V);  $V_c$ - capacitor voltage (V);  $V_{dc}$ -input dc voltage (V);  $T_1$ - non-shoot through period (s);  $T_0$ - shoot through period(s);  $T$ - total switching period (s)=  $T_0 + T_1$

Capacitor voltage of z-source network is given as

$$V_c = \frac{T - T_1}{T - T_1 - T_0} V_{dc} \quad \dots(9)$$

$$V_c = \frac{1 - \frac{T_0}{T}}{1 - 2\frac{T_0}{T}} V_{dc} \quad \dots(10)$$

$$V_c = \frac{1 - D}{1 - 2D} V_{dc} \quad \dots(11)$$

$D$ -duty cycle=  $T_0/T$

Peak dc link voltage  $V_i$  appearing across inverter input is

$$V_i = V_c - V_L = V_c - V_{dc} + V_c = 2V_c - V_{dc} \quad \dots(12)$$

$$= 2 \left( \frac{T_1}{T_1 - T_0} \right) V_{dc} - V_{dc} \quad \dots(13)$$

$$= \frac{T}{T_1 - T_0} V_{dc} \quad \dots(14)$$

$$V_i = B V_{dc} \quad \dots(15)$$

$B$ - Boost factor of inverter, where

$$B = \frac{T}{T_1 - T_0} = \frac{1}{\frac{T_1 - T_0}{T}} = \frac{1}{\frac{T - T_0 - T_0}{T}} = \frac{1}{1 - \frac{2T_0}{T}} \quad \dots(16)$$

### 3.2 ANALYSIS AND DESIGN OF THE IMPEDANCE NETWORK:

Impedance network can be redrawn like a bridge and is as shown in Figure 6. The purpose of inductor is to limit the current ripple through the

devices and thus during shoot through period  $V_L = V_c$ .

From Figure 6 assuming current  $I_2 = 0$ , current  $I_1$  entering bridge from node point 1 and divides equally between the two arms of the bridge.

From Kirchoff's laws

$$I_1 \times \frac{L}{2} + V_{dc} = \frac{I_1}{2C} \quad \dots(17)$$

$$V_{dc} = \frac{I_1}{2C} - I_1 \times \frac{L}{2} \quad \dots(18)$$

$$V_{dc} = \frac{I_1}{2} \left[ \frac{1}{C} \times L \right] \quad \dots(19)$$

The average inductor current is given as:

$$\bar{I}_L = \frac{P}{V_{dc}} \quad \dots(20)$$

where

$P$  - total power (W);  $V_{dc}$  - input voltage (V)

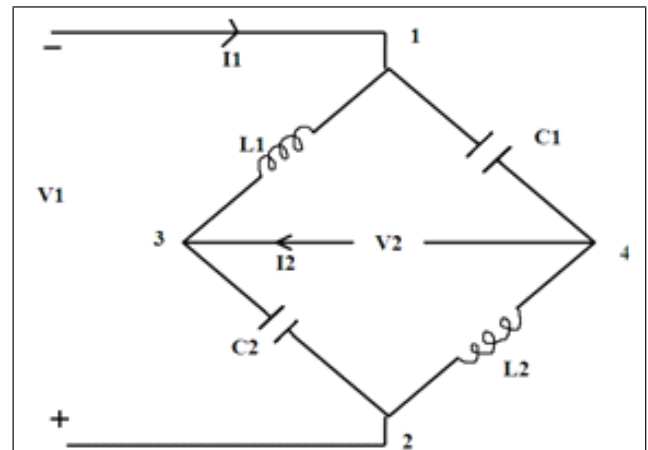


FIG. 6 IMPEDANCE NETWORK CIRCUIT- REDRAWN INDUCTOR VALUE CAN BE GIVEN AS

$$L = \frac{V_L \times T_0}{\Delta I} \quad \dots(21)$$

$\Delta I$ - inductor ripple current (A) (= maximum  $I_L$ - minimum  $I_L$ )

The capacitor value can be calculated from the equation as

$$C = \frac{\bar{I}_L \times T_0}{\Delta V_C} \quad \dots(22)$$

### 4.0 PROPOSED MPPT CONTROLLER INTEGRATED WITH OCC METHOD

OCC working can be explained from the Figure 7 & its operating waveforms are as shown in Figure 8.

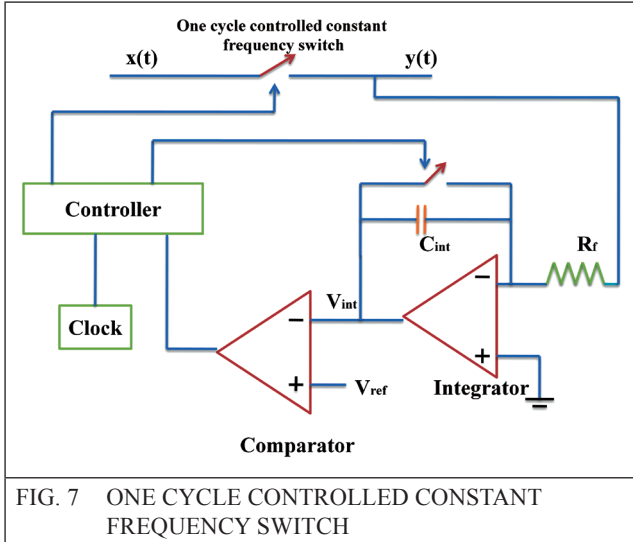


FIG. 7 ONE CYCLE CONTROLLED CONSTANT FREQUENCY SWITCH

The switch function is given as  $k(t)$

$$k(t) = \begin{cases} 1, & 0 < t < T_{ON} \\ 0, & T_{ON} < t < T_S \end{cases}$$

where  $T_{ON}$  – Switch on duration;  
 $T_{OFF}$  – Switch off duration;  $T_S = T_{ON} + T_{OFF}$ ,  
 total switching period;  $D = T_{ON} / T_S$ , duty ratio.

From Figure 5,

$$y(t) = k(t).x(t) \quad \dots(23)$$

The average of switched variable is

$$\bar{x}(t) = \frac{1}{T_S} \int_0^{T_{ON}} x(t) dt \quad \dots(24)$$

By modulating the switch duty ratio, the switch integration variable at the switch output is exactly equal to the integration value of control reference in each cycle i.e.

$$\int_0^{T_{ON}} x(t) dt = \int_0^{T_{ON}} V_{ref}(t) dt \quad \dots(25)$$

Then

$$y(t) = \frac{1}{T_S} \int_0^{T_{ON}} x(t) dt = \frac{1}{T_S} \int_0^{T_{ON}} V_{ref}(t) dt \quad \dots(26)$$

$$y(t) = V_{ref}(t)$$

As seen in Figure 7, OCC circuit comprises of an integrator reset switch, a comparator, a flip-flop, a clock and an adder. The moment switch is on; integrator starts operating at a fixed frequency clock pulse.

The integration value is given as

$$V_{int} = k \int_0^t x(t) dt \quad \dots(27)$$

$k$  – constant

when  $V_{int}$  reaches the control reference  $V_{ref}$ , the controller sends a command to the switch to change it from on state to off state. The duty ratio of present cycle is determined by equation,

$$k \int_0^{T_S} x(t) dt = V_{ref}(t) \quad \dots(28)$$

The average value of the switched variable at the switch output is given by

$$\begin{aligned} y(t) &= \frac{1}{T_S} \int_0^{dT_S} x(t) dt = \frac{1}{kT_S} V_{ref}(t) \quad \dots(29) \\ &= k_c V_{ref}(t) \end{aligned}$$

Where  $k_c = \frac{1}{kT_S} \quad \dots(30)$

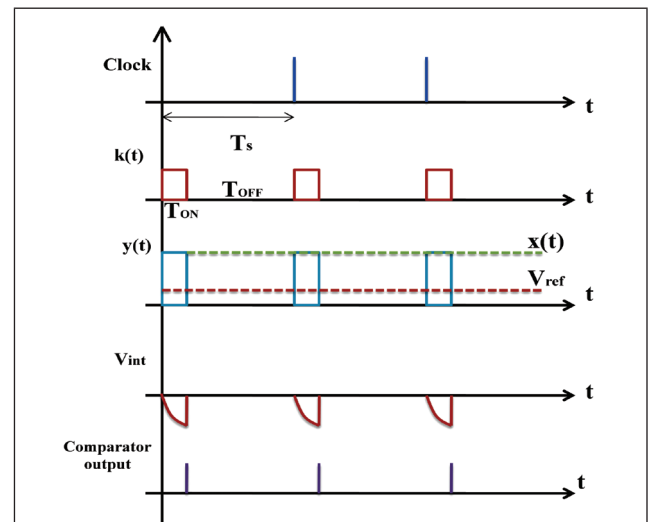


FIG. 8 OPERATING WAVWFORMS OF ONE CYCLE CONTROL

## 5.0 STABILITY ANALYSIS

The proposed single phase ZSI control has two loops, the OCC PWM modulation loop that determines the duty ratio for sinusoidal current generation in a switching cycle-by-cycle fashion and the MPPT outer loop that determines the output power according to the maximum power point of the PV array with much lower speed compared to the OCC loop.

The input-output relationship is determined by (31)

$$V_o = V_{dc}D \quad \dots(31)$$

Where D- duty ratio;  $V_{dc}$ - PV module voltage (V)

To achieve unity power factor (PF),

$$R_s \cdot i_o = K \cdot V_o - V_m \cdot D \quad \dots(32)$$

Where K- a constant;  $V_m$  ( $V_m > 0$ ) – constant during each line cycle

Unity PF can be achieved by controlling current to satisfy (32), which can be implemented using OCC technique as shown in Figure 8. Also,

$$V_{ref} = R_s \cdot i_o \quad \dots(33)$$

$$V_{int} = KV_o - V_m (t/T_s) \quad (\text{at } t = DT_s) \quad \dots(34)$$

The output power  $P_o$  of inverter is a function two parameters:  $K$  (determines the upbound of  $i_o$  & thus the maximum output power),  $K$  &  $V_m$  together (determines real power)

From (31) & (32), output power

$$P_o = V_o I_o = \frac{V_o^2}{R_s} \left( K - \frac{V_m}{V_{dc}} \right) \quad \dots(35)$$

$K$  is fixed according to the output level while  $V_m$  is adjusted according to environmental factors to determine MPPT.

From Figure 8, during time 0 to  $T_{ON}$  ( $DT_s$ ),  $V_m$  using OCC is given by

$$V_m = \frac{V_c - K_g V_{dc}}{R_f C_{int}} T_s \quad \dots(36)$$

Substituting (36) into (35), the output power will be,

$$P_o = \frac{V_o^2}{R_s} \left( K + \frac{K_g T_s}{R_f C_{int}} - \frac{V_c T_s}{V_{dc} R_f C_{int}} \right) \quad \dots(37)$$

The output power characteristics with regard to  $V_{dc}$  can be obtained from above equation (37).

The level of  $P_o$  is adjusted according to PV voltage  $V_{dc}$  and accurate MPPT can be achieved.

OCC is a non-linear process; therefore, the Poincare method [11] is used to analyze the stability. The map from the  $n^{\text{th}}$  cycle to  $(n+1)^{\text{th}}$  cycle is

$$d_{n+1} = \frac{M_2}{M_c + M_1} + \mu d_n \quad \dots(38)$$

where  $d_{n+1}$  is the duty ratio of  $(n+1)^{\text{th}}$  cycle,  $d_n$  is duty ratio of  $n^{\text{th}}$  cycle, and stability factor,  $\mu$  is given by

$$\mu = \frac{M_c - M_2}{M_c + M_1} \quad \dots(39)$$

When  $|\mu| < 1$ , the nonlinear system is stable. For a buck converter,

$$\begin{aligned} M_1 &= \frac{V_{dc} - V_o}{L} R_s \\ M_2 &= \frac{V_o}{L} R_s \\ M_c &= \frac{V_m}{T_s} \end{aligned} \quad \dots(40)$$

After substitution (39) & (40) into (38),

$$V_m > \frac{(2V_o - V_{dc})R_s T_s}{2L} \quad \dots(41)$$

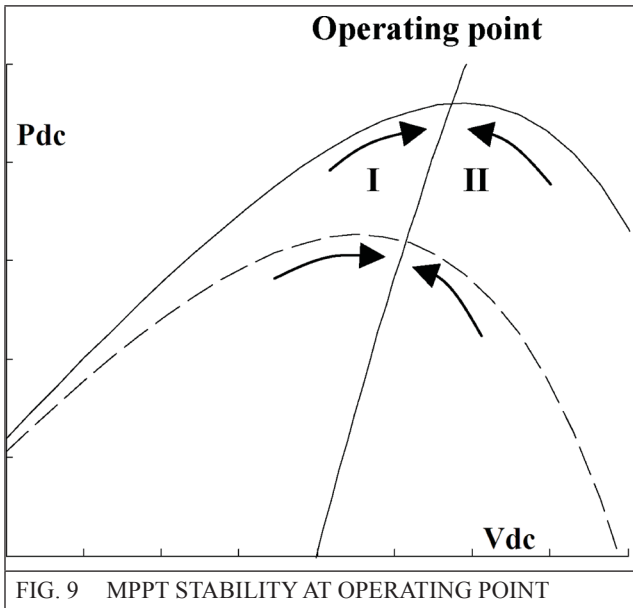
Substituting (36) into (40), it can be seen that  $V_c$  has a minimum value for the system stability

$$V_{c.min} = \frac{(2V_{o,max} - V_{dc})R_s R_f C_{int}}{L} + K_g V_{dc} \quad \dots(42)$$

$V_{c.min}$  can vary according to the maximum value of  $V_{dc}$ ,  $K_g$ ,  $R_s$  and  $R_f C_{int}$ . In proposed system, since  $R_f C_{int} \ll L$ ,  $V_{c.min}$  is mainly determined by  $K_g V_{dc}$ . If  $V_{c.min}$  is positive value, satisfying stability criterion (41) with good margin.

The stability of the outer MPPT loop can be explained with the help of Figure 9. From (36), it is derived that

$$\Delta V_m = -\frac{T_s}{R_f C_{int}} K_g \Delta V_{dc} \quad \dots(43)$$



Thus, a small change in the PV array voltage  $V_{dc}$  will cause  $V_m$  to change in the opposite direction, resulting in a change in the output power  $P_o$ . Therefore the circuit operation is stable around MPP. If the operating point is moved to left into region I from MPP point due to small perturbation,  $V_{dc}$  decreases. According to (43), when  $V_m$  is increased,  $i_o$  decreases. For this small perturbation,  $V_o$  does not change,  $P_o$  decreases while  $P_{dc}$  does not drop much. Since the input power is larger than the output power  $V_{dc}$  tends to increase, which pulls the operating point back to the original point. Similarly, if perturbation makes operating point to move in the region II,  $V_{dc}$  increases. This causes  $V_m$  to decrease, and initiates large increase in  $i_o$  and power  $P_o$  while  $P_{dc}$  does not increase. As a result,  $V_{dc}$  on capacitor tends to decrease pulling the operating point to its original MPP point. Therefore the system

inherently converges to the operating point around the maximum power point.

Circuit parameters design:

i) PV array voltage  $V_{dc}$

The main circuit is designed to be a buck converter, thus the PV voltage should be greater than the peak of the output ac voltage  $\sqrt{2}V_{o(rms)}$ . Considering a 10% variation of the rated grid voltage, it is necessary that  $V_{dc.min} \geq 250.3V$  (for 220 V grid system). Thus the irradiance is large enough (e.g. over 200 W/m<sup>2</sup>), the circuit will work at operating point determined by  $P_{dc}$  and  $P_o$ . Under cloudy weather or during sunrise or sunset, when PV voltage  $V_{dc}$  is below  $\sqrt{2}V_{o(rms)}$ , solar energy can be effectively used. However, with more PV panels connected in series, this uncontrollable area becomes negligible and does not have significant affect on the total efficiency of the system.

ii) Parameters  $K$ ,  $R_s$ ,  $V_m$

Since  $KV_o$ , determines the up-bound of  $i_o R_s$ ,  $K$  is usually chosen as large as possible so as to get the maximum flexibility of  $P_o$  with some control core. For given commercial operation amplifier with its unsaturated output swing voltage of  $V_{op(max)}$ , the value for  $K$  is chosen as  $K \leq V_{op(max)} / \sqrt{2}V_{o(rms)}$ . In this paper,  $K$  is 0.075 with the consideration of the variation of  $V_o$  and good linearity.

The upbound of  $P_o$  is determined by  $KV_o$  and  $R_s$

$$P_{o(upbound)} = V_o I_{o(upbound)} = \frac{KV_o^2}{R_s} \quad \dots(44)$$

Since  $K$  is fixed,  $R_s$  reflects the output power level. Usually,  $R_s$  is chosen according to the maximum output power.  $R_s = 1.82\Omega$ , which is chosen around the value given around the value given by (44).

According to (32) considering the worst case when  $i_o=0$ ,  $V_m$  should be large enough for the integration to meet the signal of  $KV_o$  within one switching cycle. Thus,

$$V_{m.max} = \frac{\sqrt{2}KV_{o(rms)}}{D_{max}} \quad \dots(45)$$

### iii) Parameters $R_f$ , $C_{int}$ , $V_c$ , $K_g$

According to (36) and the stability analysis,  $(T_s/R_f C_{int}) > 1$ . A high ratio enables the stable operation and limit the operating voltage change within a small range.  $K_g$  reflects the response speed controller with respect to the change of irradiance. In addition to the stability criteria condition of (42), they should also satisfy (45) as

$$\frac{V_c - K_g V_{dc}}{R_s C_1} T_s \geq \frac{\sqrt{2} K V_{o(rms)}}{D_{max}} \quad \dots(46)$$

Since there are unlimited solutions to the boundary conditions  $R_f$ ,  $C_{int}$ ,  $V_c$  and  $K_g$  are usually determined in simulation to get best approach of MPPs.

## 6.0 RESULTS

ZSI using OCC technique for MPPT is simulated in MATLAB. The parameters values used in simulation is as tabulated in Table 1 below

TABLE 1	
PARAMETER VALUES	
Parameter	Value
$V_{grid}$	220 $V_{rms}$
Grid Frequency	50 Hz
PV module voltage	250 V
$L_1, L_2$	1 mH
$C_1, C_2$	2600 $\mu$ H
$V_c$	6.2 V
$K_g$	0.042
$R_s$	1.78 $\Omega$
K	0.073
$R_f, C_{int}$	2.82 $\mu$ s

The output voltage and current waveforms obtained from simulation of 1 kW ZSI using OCC technique for MPPT control is as shown in Figure 10.

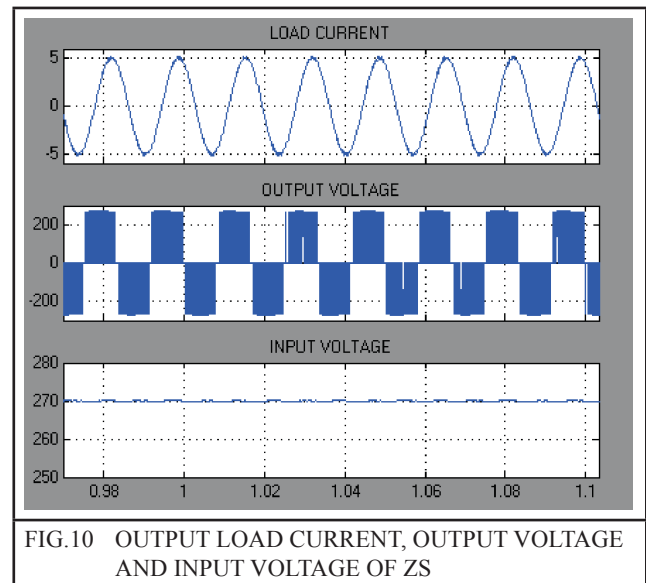


FIG.10 OUTPUT LOAD CURRENT, OUTPUT VOLTAGE AND INPUT VOLTAGE OF ZS

## 7.0 CONCLUSION

The conclusions of Simulation of 1 KW single stage transformerless ZSI with MPPT based on OCC technique for grid-tied roof top system are as listed below:

- Validation of the results by simulation in MATLAB. This method shows a great promise for reducing the complexity and thus lowering the cost and increasing the reliability for commercial & residential PV systems.
- The MPPT controller is able to automatically adjust the operating point of the PV system to the maximum power point.
- Output current of the inverter is sinusoidal with unity power factor.
- With the use of z-source inverter topology, inverter losses are reduced to great extent in comparison with traditional inverter topologies which require an additional dc-dc converter for MPPT tracking since less number of components is used.
- One cycle control circuit is not very complex compared to other MPPT controls algorithm and practical implementation is easy.
- Z-source inverter topology can be used in stand- alone systems with sufficient battery back-up, UPS, motor drive applications etc.

## 8.0 ACKNOWLEDGEMENT

The work is supported by Central Power Research Institute (CPRI), Bangalore, India. The studies were carried out in the solar PV and inverter testing laboratory of Energy Efficiency and Renewable Energy Division, CPRI Bangalore and the Research works are done with the guidance of the experts from the Organization.

## 9.0 REFERENCES

- [1] J. M. Carrasco, L. G. Franquelo, J. T. Bialaisiewicz, E. Galvan, R. C. Portillo Guisado, M. A. M. Prats, J. I. Leon, and N. Moreno-Alfonso, "Power-electronic systems for the grid integration of renewable sources: A survey", *IEEE Trans. Ind. Electron.*, vol. 53, no.4, pp.1002-1016, Jun. 2006
- [2] S. B. Kjaer, J. K. Pedersen, and F. Blaabjerg, "A review of single-phase grid-connected inverters for photovoltaic modules", *IEEE Trans. Ind. Appl.*, vol. 41, no.5, pp. 1292-1302, Sep./ Oct. 2005
- [3] T. Shimizu, O. Hashimoto, and G. Kimura, "A novel high-performance utility interactive photovoltaic inverter system", *IEEE Trans. Power electronic.*, vol.18, no.2, pp. 704-711, Mar. 2003.
- [4] W. Tsai-Fu, N. Hung-Shou, H. Hui-Ming, and S. Chih-Lung, "PV power injection and active filtering with amplitude clamping and amplitude scaling algorithms", *IEEE Trans. Ind. Appl.*, vol. 43, no. 3, pp. 731-741, May/ Jun. 2007.
- [5] Peng, F. Z., Joseph, A., Wang, J., et al: "Z-source inverter for motor drives", *IEEE Trans. Power Electron.*, Vol. 20, No. 4, pp. 857-863, 2005.
- [6] Huang, Y., Shen, M., Peng, F.Z., Wang, J., "Z-source inverter for residential photovoltaic systems", *IEEE Trans. Power Electron.*, Vol. 21, No. 6, pp. 1776-1782, 2006.
- [7] Rosas-Caro, J.C., Peng, F.Z., Cha H., Rogers C, "Z-source converter-based energy-recycling zero-voltage electronic loads", *IEEE Trans. Ind. Electron.*, Vol. 56, No. 12, pp. 4894-4902, 2009.
- [8] Jingbo, L., Jiangang, H., Longya, X., "Dynamic modeling and analysis of Z source converter-derivation of AC small signal model and design-oriented analysis", *IEEE Trans. Power Electron.*, Vol. 22, No. 5, pp. 1786-1796, 2007.
- [9] Keyue M. Smedley, Slobodan Cuk, "One-cycle control of switching converters", *IEEE Trans, power electronics*, vol. 10, no. 6, pp.625- 633, Nov. 1995
- [10] Yang Chen, Keyue Ma Smedley, "A cost effective single- phase inverter with maximum power point tracking", *IEEE Trans, power electronics*, vol. 19, no. 5, pp.1289-1294, Sept. 2004
- [11] Y. Chen, K. Smedley, F. Vacher, J. Brouwer, "A new maximum power point tracking controller for photovoltaic power generation", *IEEE trans*, vol. 1, pp. 58-62, Feb. 2003.

